ARTICLES SCIENCE CHINA Materials

mater.scichina.com link.springer.com

Published online 29 February 2016 | doi: 10.1007/s40843-016-0123-0
Sci China Mater 2016, 59(2): 112–121

A mixed-solvent route to unique PtAuCu ternary nanotubes templated from Cu nanowires as efficient dual electrocatalysts

Qi-Qi Fu†, Hui-Hui Li†, Si-Yue Ma, Bi-Cheng Hu and Shu-Hong Yu*

ABSTRACT **Forming alloys with transition metal remarkably decreases the usage of noble metal and offers benefits for electrocatalysis. Here we introduced a mixed-solvent strategy to synthesize unique PtAuCu ternary nanotubes (NTs) with porous and rough surface, using high quality Cu nanowires (NWs) as the partial sacrificial templates. We found that Au plays a key role in the enhancement of electrocatalytic performance for both methanol oxidation reaction (MOR) and formic acid oxidation reaction (FAOR). The mass activities of PtAuCu NTs after acid leaching for MOR and FAOR reach 1698.8 mA mg^{-1}_{Pt} at 0.9 V and 1170 mA mg^{-1}_{Pt} at 0.65 V, respectively. Such ternary NTs show impressive stability due to the irreversibly adsorption of CO* on the Au surface instead of the active Pt surface and the excellent structure stability. The present method could be extended to prepare other new multi-functional electrocatalysts.**

Keywords: ternary alloy, nanotube, electrocatalysis, methanol oxidation reaction, formic acid oxidation reaction, copper nanowire

INTRODUCTION

Direct methanol fuel cells (DMFCs) and direct formic acid fuel cells (DFAFCs) play important roles in the development of renewable energies to mitigate the global warming and reduce our dependence on fossil fuels [1–3]. Methanol and formic acid are easier to store in small electronics and portable power than high-pressure hydrogen. Compared with ethanol, they do not require the catalytic breakage of C–C bond, which will hinder the kinetics [4]. As we know, pure Pt materials are the most promising anode or cathode catalysts applied in a wide range of DMFCs and DFAFCs [2,5–7]. However, considering the low abundance, high price of Pt, and the strong poison from CO* intermediate species, design and synthesis of novel Pt-based electrocatalysts with low cost and excellent performance is still critical [2].

Forming Pt-based alloys with transition metal is a potent strategy to remarkably reduce the usage of noble metal, and therefore enhance the catalytic activity [8–19]. For alloy catalysts, the different arrangements of dissimilar atoms on the surface or subsurface could modify the electronic structure [20,21] and induce compression [22] or expansion [20] of the lattice [23], in other words, ligand effects and strain effects. Strasser *et al.* [24] observed that the PtCu core-shell structure shows compressive strain, which results in weakened chemisorption of oxygenated species and enhanced catalytic activity. Stamenkovic *et al.* [25] reported that the (111) facets with the same surface composition and arrangement but with different d-band center, resulted in different binding energy of the intermediate on the surface to influence the kinetics. Besides, electrocatalysts with open surface, for example, concave structure [26], high-index facets [27], nanoframes [5] and nanodendrite [28], commonly show extraordinary electrocatalytic performance. Coupling such shape-controlled synthesis with post-treatments is an effective strategy to prepare effective and highly active catalysts. As a general post-treatment, acid leaching is the main method [29–32] to form active and rough skeleton surface. Compared with other post-treatments, acid leaching has the following advantages: (a) acid can remove some specific surfactants used in soft-template synthesis; (b) acid leaching does not decrease the dispersing ability; (c) acid leaching is milder, simpler and more practical [32,33].

Furthermore, compared with zero-dimensional (0D) materials, one-dimensional (1D) materials are thought to alleviate all natural drawbacks of 0D materials for enhancing stability. The Ostwald ripening [34], support break-

Division of Nanomaterials & Chemistry, Hefei National Laboratory for Physical Sciences at the Microscale, Collaborative Innovation Center of Suzhou Nano Science and Technology, Department of Chemistry, Chinese Academy of Sciences (CAS) Center for Excellence in Nanoscience, Hefei Science Center of CAS, University of Science and Technology of China, Hefei 230026, China
† These authors contributed equally to this work.
* Corresponding author (email: shyu@ustc.edu.cn)

down and irreversible oxidation [35] of 0D catalysts are ascribed to the decomposition of the defect sites and lattice boundary. Moreover, 1D electrocatalysts are easier to assemble into 2D or 3D network, improving structure stability. It is worth mentioning that our group has done many pioneering works on the assembly of nanowires (NWs) [36]. Among the reported methods [16,37–40], sacrificial template method based on galvanic replacement reaction is facile, general, effective and applicable to prepare 1D structure electrocatalysts. Nonetheless, the quality of products is limited by the quality of the templates, the preparation skills and the production scale. To solve these barriers, our group developed some high quality templates like Te NWs [41,42] and Cu NWs [39], but the removal of surfactant and prevention of oxidation of Cu NWs are still challenging.

Herein, we report a mixed-solvent strategy coupled with a simple galvanic replacement reaction to prepare uniform self-supported PtAuCu ternary nanotubes (NTs) with controllable composition using Cu NWs as sacrificial templates. As the least reactive metal, Au is inactive for methanol oxidation reaction (MOR), but promotes the stability of the alloyed catalysts to a large extent. AuCu nanoparticles (NPs) were found to have bifunctional catalytic sites for efficient catalysis for CO oxidation implying less catalysts poisoning [43]. The hollow structure inherited from Cu NWs can be explained by Kirkendall effect [44]. Compared with NW structure, NT structure is in favor of mass transport and higher atom utilization of noble metal, providing more active sites both in the internal and external tube wall. After acetic acid (AA) treatment, the PtAuCu-AA NTs with porous and rough surface were efficient and stable for both MOR and formic acid oxidation reaction (FAOR). Test results further demonstrate the excellent catalytic performance benefited from unique morphology relative to reported catalysts with the same composition but different structure [45–47]. The MOR and FAOR mass activities of $Pt_{27}Au_3Cu$-AA NTs were nearly 3.9 and 7.3 times higher than that of commercial Pt/C, respectively. Additionally, long-term stability tests showed that the $Pt_{27}Au_3Cu$-AA NTs exhibit superior stability for both MOR and FAOR.

EXPERIMENTAL SECTION

Materials

$CuCl_2{\cdot}2H_2O$, glucose, dimethyl sulfoxide (DMSO), isopropanol, methanol, toluene, cyclohexane, $HAuCl_4{\cdot}4H_2O$, sulfuric acid, perchloric acid, formic acid were all from Shanghai Chemical Reagent Co. Ltd; hexadecylamine (HDA) and Nafion were from Sigma–Aldrich; platinum (II) chloride was from J&K Chemical Ltd. All chemical reagents were used without any further purification.

Instruments

Scanning electron microscopy (SEM) image was taken using a Zeiss Supra 40 scanning electron microscope at an acceleration voltage of 5 kV. Transmission electron microscopy (TEM) and high resolution TEM (HRTEM) images were obtained on JEOL-2100F TEM instrument. High resolution high angle annular dark-field scanning TEM (HAADF-STEM), energy dispersive spectrometer (EDS), elemental mapping images and line-scan analysis image were obtained on JEM-ARM 200F. Power X-ray diffraction (XRD) data were recorded from a Philips X'Pert PRO SUPER X-ray diffractometer equipped with graphite mono-chromatized Cu Kα radiation (λ=1.54056 Å). X-ray photoelectron spectra (XPS) was determined by an X-ray photoelectron spectrometer (Thermo ESCALAB 250) with an excitation source of Al Kα radiation (1486.6 eV). Inductively coupled plasma (ICP) data was obtained by using an Optima 7300 DV instrument. Electrochemical measurements were carried out with a three electrode system on an IM6ex electrochemical workstation (Zahner, Germany).

Synthesis of Cu NWs

Cu NWs were synthesized through a modified hydrothermal method. Firstly, 85.5 mg $CuCl_2{\cdot}2H_2O$, 99.0 mg glucose and 0.54 g HDA were dissolved in 40 mL deionized (DI) water by vigorous magnetic stirring for 5 h to form a sky-blue emulsion. Then, the emulsion was transferred into a 100 mL polytetrafluoroethylene-linked stainless-steel autoclave and reacted in an oven at 120°C for 24 h. After the synthesis, the Cu NWs were centrifuged at 2000 rpm and washed with DI water for two times to eliminate the particles from the emulsion. Finally, Cu NWs were collected by cyclohexane and quantified by ICP. The dispersed solution was stored in the fridge before using.

Synthesis of PtAuCu NTs

For example, a suspension contained 60 μmol Cu NWs in DMSO and toluene mixed solution was ultrasonic processed to disperse well. Then, after refluxing (120°C, 5 min) in a 100 mL three-neck flask with nitrogen gas bubbling, 27 μmol $PtCl_2$ and 3 μmol $HAuCl_4{\cdot}4H_2O$ were added into the system under vigorous magnetic stirring and reacted for 2 h. According to the molar amount of the precursors, we named the product as $Pt_{27}Au_3Cu$ NTs.

Electrochemical measurement

Before measuring, the catalysts were centrifuged and sus-

pended in 25 mL acetic acid at 60°C overnight with magnetic stirring. After that, the catalysts were washed with isopropanol twice before dispersing. Nafion (0.5% *v*/*v*) was added and the dispersion was sufficiently sonicated.

Five micrograms NTs were dropped on a rotation disk electrode (RDE) with a polished glassy carbon surface (PINE, 5 mm in diameter). Surface cleaning and restructuring was carried out by cyclic voltammetry (CV) scanning in N_2-saturated 0.1 mol L^{-1} $HClO_4$ solution at room temperature between −0.25 and 1.00 V (*vs*. Ag/AgCl) at a sweep rate of 250 mV s^{-1}. The electrochemical surface area (ECSA) was calculated by integrating the hydrogen-adsorption charge in the CV scans. MOR was measured in N_2-saturated 0.5 mol L^{-1} H_2SO_4 and 1 mol L^{-1} methanol mixed solution at room temperature between −0.20 and 1.00 V with a sweep rate of 50 mV s^{-1}. The stability was studied by chronoamperometry at 0.55 V (*vs*. Ag/AgCl). FAOR was measured in N_2-saturated 0.5 mol L^{-1} H_2SO_4 and 0.5 mol L^{-1} HCOOH mixed solution at a sweep rate of 50 mV s^{-1} between −0.25 and 1.0 V. The stability was measured by chronoamperometry at 0.2 V (*vs*. Ag/AgCl). All of the electrode potentials were recorded with Ag/AgCl electrode and calibrated by a reversible hydrogen electrode (RHE).

RESULTS AND DISCUSSION

To obtain low-Pt-content 1D PtAuCu NTs, we used high-quality Cu NWs with uniform size as partial sacrificial templates. SEM image in Fig. 1a shows that uniform and well-crystallized Cu NWs with high aspect ratio and good electron conductivity can be prepared via our previous reported method with minor modification [39]. The Cu NWs were dispersed in cyclohexane (insert of Fig. 1a) and stored in refrigerator. The HDA served as surfactant is important to the 1D structure formation and protection of the Cu NWs. The absorption of HDA on the surface prevented the Cu NWs from oxidation and enhanced the dispersibility in some specific organic solvents. These HDA-protected Cu NWs can be stored for at least one year without any oxidation. Fig. S1 shows the TEM images and XRD pattern of newly prepared Cu NWs and stored Cu NWs for half a year or one year. Obviously, there is no CuO or Cu_2O phase found in the XRD pattern. However, HDA will hinder the following galvanic replacement reaction to a certain extent. To solve this problem, redundant HDA was removed through a tedious step in previous works [39,40]. This removing process results in inevitably undesired partial oxidation and loss after alternately washing with hexane and ethanol for several times. It is expected that the HDA-protected Cu NWs could be used as sacrificial templates directly. Therefore, finding a proper solution system that can possibly disperse the HDA-protected Cu NWs is important and advantageous to the following galvanic replacement reaction.

We designed a very suitable reaction system composed of toluene and DMSO using the unwashed HDA-protected Cu NWs as the templates directly. Toluene is a good solvent for HDA, it can accelerate the reaction rate, but is not favorable for the control of the morphology. In contrast, as a poor solvent, DMSO is beneficial to improve the morphology, since it can slow down the reaction rate by control the reaction probability for the solvation of noble metal precursors. So optimizing a volume ratio of such two solvents is important for the successful synthesis of PtAuCu NTs.

The PtAuCu NTs were prepared by adding $PtCl_2$ and $HAuCl_4{\cdot}4H_2O$ into the mixed solvent (toluene and DMSO) at 120°C. By changing the amount of Pt and Au precursors, a series of PtAuCu NTs with different composition were prepared. The PtAuCu NTs were named according to the added molar amount (μmol) of the precursors. The corresponding actual molar ratio of the products, containing bulk composition (ICP data) and surface composition (XPS data), were listed in Table S1. The atomic ratio of Au component near the surface is lower than that in bulk, indicating that the core-shell like structure was formed. The formation of core-shell like structure is ascribed to the higher reaction rate of the Au precursor covered by the followed deposition of Pt atoms (Table S2). Figs 1b and S2 show the typical TEM image of PtAuCu NTs with diameter between 25 and 35 nm, which is close to that of Cu NWs. Then, we removed the HDA residue on PtAuCu NTs surface and leached partial surface Cu atoms without destroying the structure by acid leaching, and we named the products as PtAuCu-AA NTs.

The porous and rough PtAuCu-AA NTs composed of single NPs with an approximately diameter of 10 nm (Fig. 1c) [5,26]. Selected area election diffraction analysis (SEAD) (Fig. S2d) proves that the PtAuCu-AA NTs are well-crystallized. The lattice parameters of the PtAuCu-AA NTs are mainly 0.214 nm, 0.185 nm and 0.131 nm (Figs 1d and e), corresponding to the (111), (200) and (220) facets (Fig. 1f), respectively. Mavrikakis *et al.* [48] reported that the Pt (111) facet prefers to oxidize methanol directly to CO_2 without CO^* as an intermediate. With adding more Au precursor, the relative intensity of Au_3Cu and Au phases increased gradually. Compared with the lattice parameter of Pt (PDF#70-2057), the PtAuCu-AA NTs exhibit a compressive strain, which is favorable for the enhancement of the electrocatalytic activity [24].

According to our test results (Fig. S3), when the molar

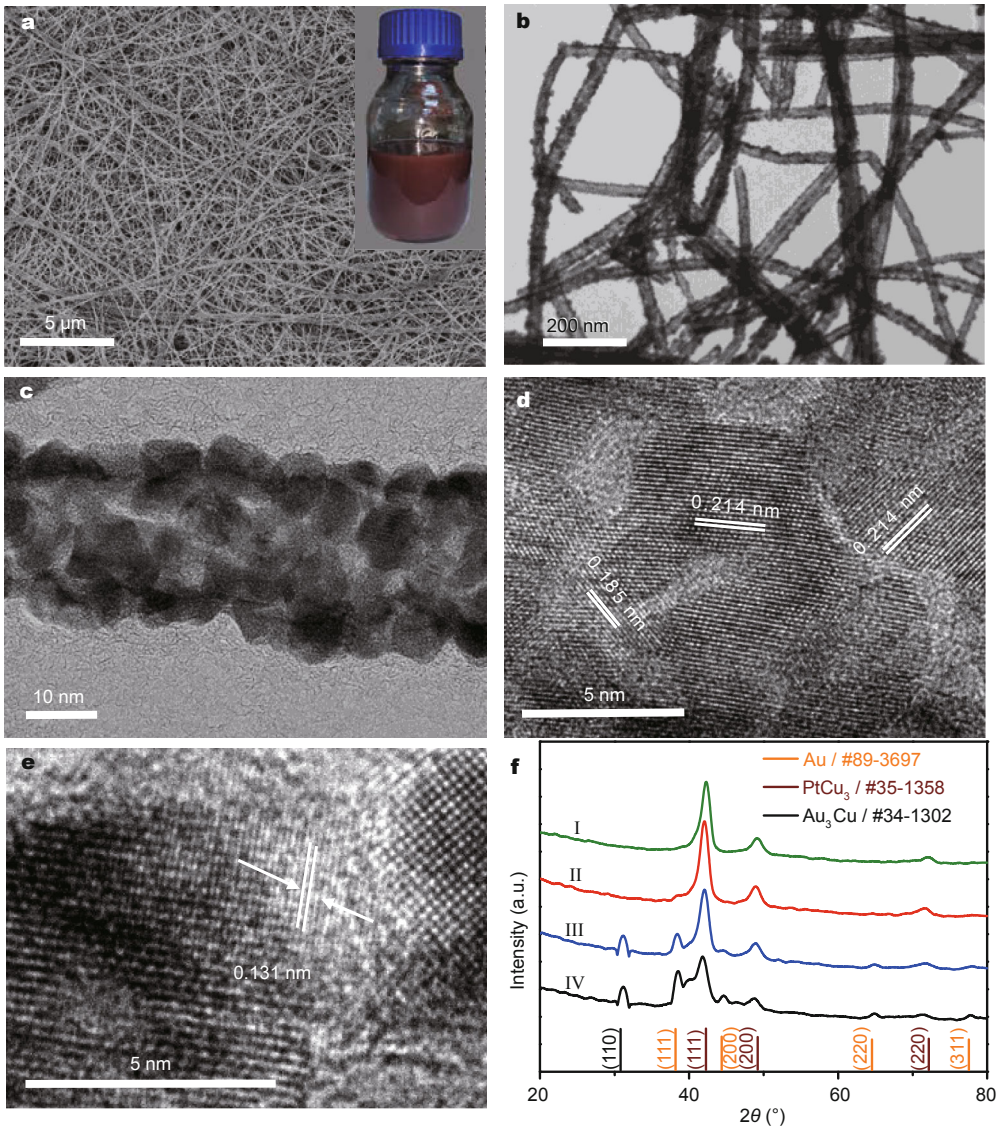

Figure 1 (a) SEM image of Cu NWs. The insert shows the Cu NWs dispersed in cyclohexane. (b) TEM image of $Pt_{27}Au_3Cu$ NTs. (c, d, and e) STEM images of $Pt_{27}Au_3Cu$-AA NTs, suggesting that, the NTs are porous and composed of single nanoparticles (ca. 10 nm in diameter). (f) XRD pattern of $Pt_{29}Au_1Cu$-AA (I), $Pt_{27}Au_3Cu$-AA (II), $Pt_{25}Au_5Cu$-AA (III) and $Pt_{20}Au_{10}Cu$-AA (IV) NTs.

ratio of total noble metal and Cu NWs was 1:2, the PtAu-Cu-AA NTs exhibite the best electrocatalytic activity. In order to obtain an optimal catalyst, we kept the added molar ratio of total noble metal to Cu NWs but changed the ratio of $PtCl_2$ and $HAuCl_4{\cdot}4H_2O$. A series of PtAuCu-AA NTs were prepared, i.e., $Pt_{29}Au_1Cu$-AA NTs, $Pt_{27}Au_3Cu$-AA NTs, $Pt_{25}Au_5Cu$-AA NTs and $Pt_{20}Au_{10}Cu$-AA NTs. As the lattice parameter difference of Au and Pt is less than that of Cu and Pt, the compressive strain is milder with the increase of the content of Au (Fig. 1f), which is presented as the negetive shift of the 2θ degree and accompanying the formation of Au and AuCu phases. However, from the XPS data (Fig. S4), it is notable that the chemical states of Pt, Cu and Au of different PtAuCu-AA NTs are almost uniform, proving the negligible electronic effect.

The line-scan analysis across a single nanoparticle on the $Pt_{27}Au_3Cu$-AA NTs (Fig. 2b) demonstrates that a very thin Pt-rich surface was formed after the acid leaching process with a confined surface processing ability [30]. The element mapping (Fig. 2c) showes that Pt, Au and Cu atoms are evenly distributed along the NTs. The rough and porous surface of the NTs is also proved by the HAADF-STEM image (Fig. 2a) more directly. This unique structure is advantageous for the enhancement of electrocatalytic

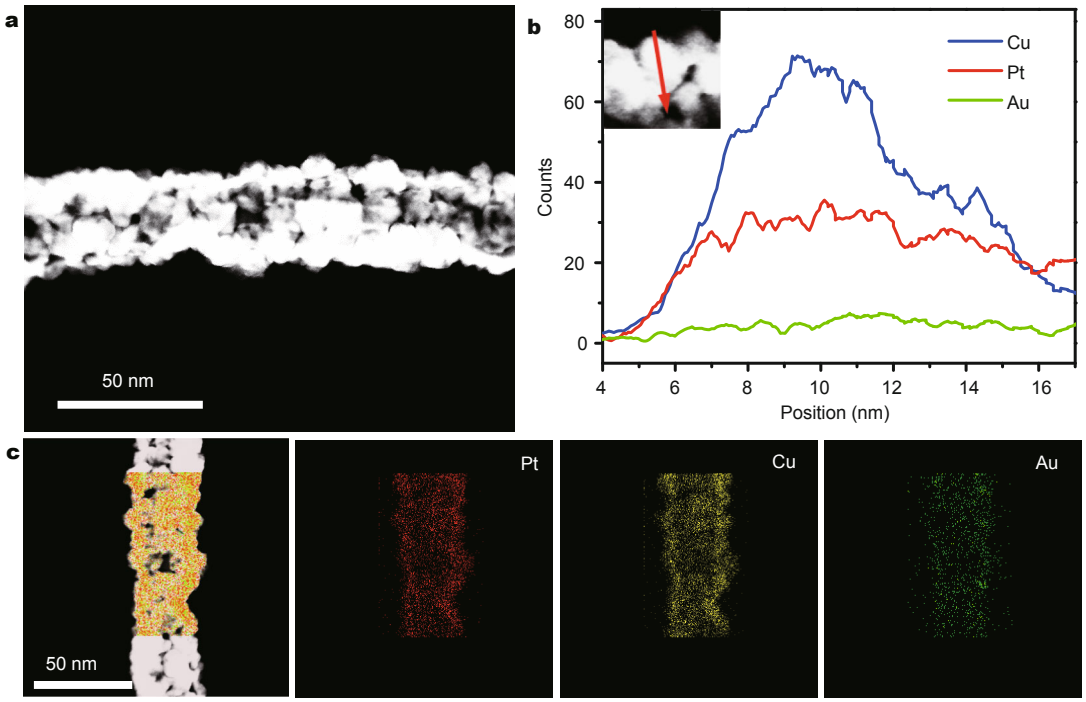

Figure 2 (a) HAADF-STEM image of the $Pt_{27}Au_3Cu$-AA NTs. (b) Line-scan analysis across a single nanoparticle on the $Pt_{27}Au_3Cu$-AA NTs. (c) Element mapping results of $Pt_{27}Au_3Cu$-AA NTs. From (b) and (c), it can be seen that the NTs are homogeneous alloys with a thin Pt-rich surface.

activity.

Besides the acid leaching, the surface leaching of Cu and the surface restructuring can be further processed by electrochemical method [49]. In this work, the catalysts were sufficiently activated after 20 potential cycles (Fig. S5). The Faradic-current peaks at 0.8V (*vs.* RHE) in the initial CV represent surface Cu dissolution from the surface or subsurface of $Pt_{27}Au_3Cu$-AA catalysts. As the voltammetric cycling continues, Cu atoms near the surface are further dissolved to form PtAu-rich surface catalysts, meeting the requirements of highly active catalysts. Fig. 3a shows the CV curves of activated PtAuCu-AA NTs. In the cathodic scan, there is a Pt–H adsorption peak between 0.05 and 0.4 V served to calculate the ECSA [50]. Interestingly, although the $Pt_{27}Au_3Cu$-AA NTs possess the smallest ECSA among the NTs, they exhibit the highest activity for MOR and FAOR, indicating the importance of the modification of Pt atoms by other alloyed atoms. It proves that not only the increase of active sites, but also the modification of Pt atoms has positive influence to enhance the catalytic performance.

The electrocatalytic activity of PtAuCu-AA NTs for MOR was studied by CV in N_2-saturated 0.5 mol L^{-1} H_2SO_4 and 1 mol L^{-1} methanol mixed solution. As shown in Fig. S6, the MOR and FAOR activity of PtAuCu NTs after acid leaching are much higher than that before acid leaching, proving the importance of acid leaching for the formation of Pt-rich surface and the removal of HDA. As shown in Figs 3b and c, we notice that the mass activities of these PtAuCu-AA NTs exhibit volcano-type dependence. The mass activity of $Pt_{27}Au_3Cu$-AA NTs reaches as high as 1698.8 mA mg^{-1}_{Pt} at 0.9 V, which is nearly 3.9 times higher than that of commercial Pt/C. The mass activities of $Pt_{29}Au_1Cu$-AA NTs, $Pt_{25}Au_5Cu$-AA NTs and $Pt_{20}Au_{10}Cu$-AA NTs are 3.1, 3.3 and 3.1 times higher than that of commercial Pt/C, respectively. Moreover, it is also better than many reported catalysts (Table S3). It is worth mentioning that under the same test conditions, with the improvement of manufacturing technology, the mass activity of commercial Pt/C tested by us is nearly two-fold higher than that of previous report [51]. The stability tests were studied by chronoamperometry at 0.76 V. From Fig. 3d, it can be seen that the $Pt_{27}Au_3Cu$-AA NTs also exhibit the best stability. This excellent performance can be partially attributed to the outstanding CO^* tolerance as characterized by the current ratio of two peaks in the forward (I_f) and backward (I_b) scans (Fig. 3b). The ratio reaches as high as 1.46, which means the quick removal of CO^* intermediate species. Compared with PtCu NTs (Fig. S7), the $Pt_{27}Au_3Cu$-AA NTs show lower activity but better stability. It is likely caused by the ensemble effects of the introduction of Au, resulting in many distinctive functions, like irreversible adsorption

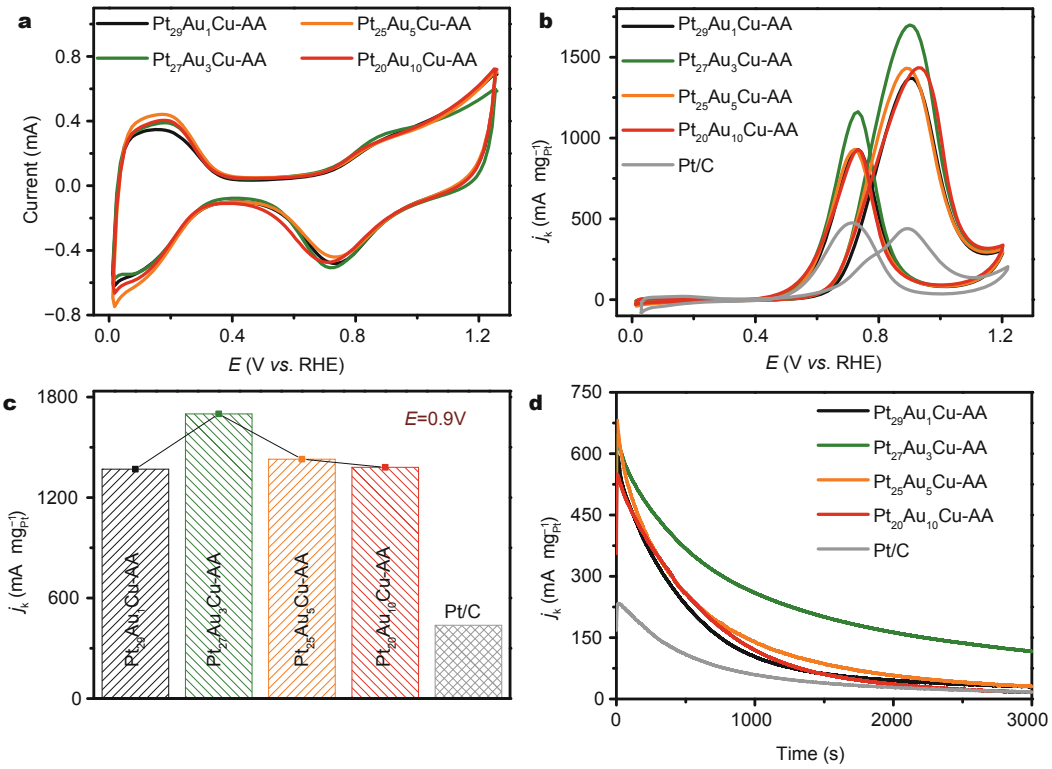

Figure 3 (a) CV curves of PtAuCu-AA NTs in N_2-saturated 0.1 mol L^{-1} $HClO_4$ solution at a sweep rate of 250 mV s^{-1}. (b) MOR curves in N_2-saturated 0.5 mol L^{-1} H_2SO_4 and 1 mol L^{-1} methanol mixed solution at a sweep rate of 50 mV s^{-1}. (c) Volcano plots. (d) Catalyst stability tests in N_2-saturated 0.5 mol L^{-1} H_2SO_4 and 1 mol L^{-1} methanol mixed solution at 0.76 V. The Pt loading was all 25.5 μg cm^{-2}.

and efficient catalysis for the oxidation of CO^* [43,52]. Although Au is inertia for MOR, there is an optimal balance for the $Pt_{27}Au_3Cu$-AA NTs between the decreased active sites [53] and the enhanced ensemble effects to obtain the highest MOR activity. This phenomenon may explain the volcano-type dependence of PtAuCu-AA NTs. What is particularly worth mentioning is that Yamauchi *et al.* [54] reported similar result that the $Pt_{90}Au_{10}$ binary alloys show best stability.

The PtAuCu-AA NTs also exhibit excellent electrocatalytic activity for FAOR. As shown in Figs 4a–c, the mass activities of $Pt_{27}Au_3Cu$-AA NTs are competitive (Table S4). They reach 1170 mA mg^{-1}_{Pt} at 0.65 V and 1650 mA mg^{-1}_{Pt} at 0.95 V, which are respectively 7.3 and 3.4 times higher than that of commercial Pt/C. It means that the PtAuCu-AA NTs are efficient for both direct and indirect pathway [7]. Since the indirect pathway is considered to be a dehydration reaction resulted in a strong adsorption of CO^* species [7], we mainly paid attention to the direct pathway. Consequently, we studied the direct pathway stabilities of the catalysts by chronoamperometry at 0.43 V. The result shows that the $Pt_{27}Au_3Cu$-AA NTs exhibit higher activity and better stability (Fig. 4d) for FAOR than that of PtCu-AA NTs and commercial Pt/C. Increasing the atom ratio of Au cannot enhance the catalyst performance for FAOR with the comparison of $Pt_{20}Au_{10}Cu$-AA NTs.

The long-term stability tests for MOR and FAOR were studied by chronoamperometry (Fig. S8). Because the mass activity of $Pt_{27}Au_3Cu$-AA NTs is considerably higher than that of commercial Pt/C, we used the relative current as the *Y*-axis to show the comparison more directly. As shown in Fig. S8, the $Pt_{27}Au_3Cu$-AA NTs exhibit superior long-term stability for both MOR and FAOR comparing with commercial Pt/C, due to more CO^* intermediate species formed on the surface of $Pt_{27}Au_3Cu$-AA NTs than that on Pt/C. More importantly, the irreversible adsorption of CO^* on the Au surface instead of the Pt surface, acting as a promoter for the reaction, can be the key factor of the enhancement of stability. Futhermore, in order to confirm the structure stability, TEM and HRTEM images show that the $Pt_{27}Au_3Cu$-AA NTs maintain porous, rough surface structure and better crystallinity after stability tests, responsible for the excellent structure stability (Fig. 5).

CONCLUSIONS

In summary, we prepared uniform, self-supported and

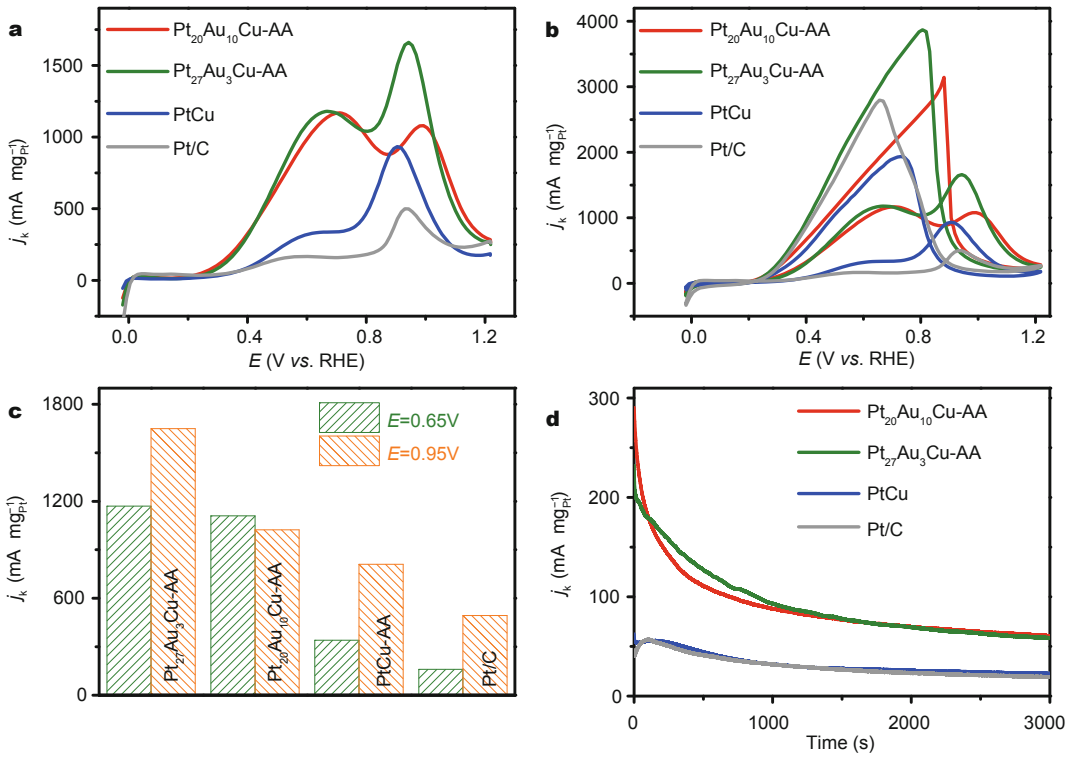

Figure 4 FAOR anodic scan curves (a), CV curves (b) and catalyst stability tests (d) at 0.43 V in N_2-saturated 0.5 mol L^{-1} H_2SO_4 and 0.5 mol L^{-1} HCOOH mixed solution at a sweep rate of 50 mV s^{-1}. (c) Mass activities of the catalysts at 0.65 V (direct pathway) and 0.95 V (indirect pathway).

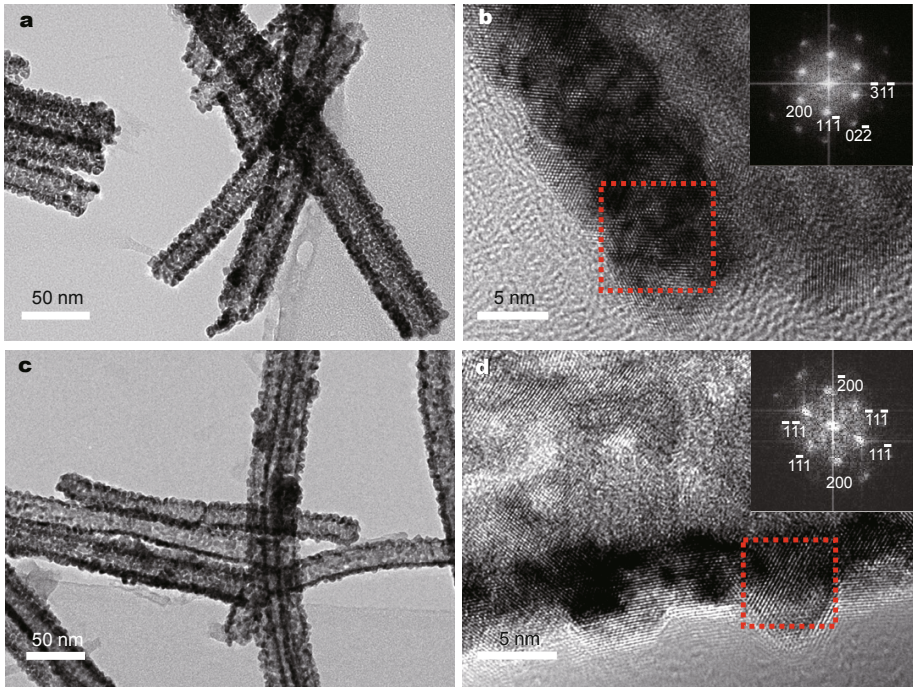

Figure 5 TEM and HRTEM images of $Pt_{27}Au_3Cu$-AA NTs after MOR (a, b) and FAOR (c, d) long-term stability tests, from which we can see that the porous and rough surface structure, and the well crystallinity were kept. Inserts of b and d show corresponding fast Fourier transform patterns, which prove that the polycrystalline NTs are composed of monocrystalline NPs.

well-crystallized PtAuCu NTs by a mixed-solvent strategy coupling with acid leaching method. The HDA-protected Cu NWs can be used as partial sacrificial templates for its scalable synthesis potential and oxidation-resistivity. The well-crystallized Cu NWs act as not only partial sacrificial templates but also efficient alloy element to optimize the catalytic performance via strain effect. A post-treatment of acid leaching plays an important role in forming rough, porous and thin Pt-rich surface core-shell like structure responsible for the excellent catalytic activity for both MOR and FAOR. Moreover, Au is the key factor to the enhancement of stability. The irreversible adsorption of CO^* on the Au surface instead of on the Pt surface and the efficient catalysis for the oxidation of CO^* can be the reasons that the PtAuCu NTs exhibit impressive stability. Such PtAuCu NTs show promising prospects for anode catalysts of DMFCs and DFAFCs. This mixed solvent strategy provides a promising strategy to realize a balance of the prevention of oxidation of Cu NWs and the blocking effect of the surfactant.

Received 31 January 2016; accepted 22 February 2016; published online 29 February 2016

1 Arico AS, Bruce P, Scrosati B, *et al*. Nanostructured materials for advanced energy conversion and storage devices. Nat Mater, 2005, 4: 366–377
2 Koenigsmann C, Wong SS. One-dimensional noble metal electrocatalysts: a promising structural paradigm for direct methanol fuel cells. Energy Environ Sci, 2011, 4: 1161–1176
3 Arico AS, Srinivasan S, Antonucci V. DMFCs: from fundamental aspects to technology development. Fuel Cells, 2001, 1: 133–161
4 Ksar F, Ramos L, Keita B, *et al*. Bimetallic palladium-gold nanostructures: application in ethanol oxidation. Chem Mater, 2009, 21: 3677–3683
5 Chen C, Kang YJ, Huo ZY, *et al*. Highly crystalline multimetallic nanoframes with three-dimensional electrocatalytic surfaces. Science, 2014, 343: 1339–1343
6 Kakati N, Maiti J, Lee SH, *et al*. Anode catalysts for direct methanol fuel cells in acidic media: do we have any alternative for Pt or Pt-Ru? Chem Rev, 2014, 114: 12397–12429
7 Jiang K, Zhang HX, Zou SZ, Cai W. Electrocatalysis of formic acid on palladium and platinum surfaces: from fundamental mechanisms to fuel cell applications. Phys Chem Chem Phys, 2014, 16: 20360–20376
8 Cui Z, Chen H, Zhao M, *et al*. Synthesis of structurally ordered Pt_3Ti and Pt_3V nanoparticles as methanol oxidation catalysts. J Am Chem Soc, 2014, 136: 10206–10209
9 Sun X, Li D, Ding Y, *et al*. Core/shell Au/CuPt nanoparticles and their dual electrocatalysis for both reduction and oxidation reactions. J Am Chem Soc, 2014, 136: 5745–5749
10 Li HH, Zhao S, Gong M, *et al*. Ultrathin PtPdTe nanowires as superior catalysts for methanol electrooxidation. Angew Chem Int Ed, 2013, 52: 7472–7476
11 Wang G, Huang B, Xiao L, *et al*. Pt skin on AuCu intermetallic substrate: a strategy to maximize Pt utilization for fuel cells. J Am Chem Soc, 2014, 136: 9643–9649
12 Jia Y, Jiang Y, Zhang J, *et al*. Unique excavated rhombic dodecahedral $PtCu_3$ alloy nanocrystals constructed with ultrathin nanosheets of high-energy {110} facets. J Am Chem Soc, 2014, 136: 3748–3751
13 Baldizzone C, Mezzavilla S, Carvalho HWP, *et al*. Confined-space alloying of nanoparticles for the synthesis of efficient PtNi fuel-cell catalysts. Angew Chem Int Ed, 2014, 53: 14250–14254
14 Chang J, Feng L, Liu C, *et al*. An effective Pd-Ni_2P/C anode catalyst for direct formic acid fuel cells. Angew Chem Int Ed, 2014, 53: 122–126
15 Chen S, Su H, Wang Y, *et al*. Size-controlled synthesis of platinum-copper hierarchical trigonal bipyramid nanoframes. Angew Chem Int Ed, 2015, 54: 108–113
16 Xia BY, Wu HB, Li N, *et al*. One-pot synthesis of Pt-Co alloy nanowire assemblies with tunable composition and enhanced electrocatalytic properties. Angew Chem Int Ed, 2015, 54: 3797–3801
17 Wu Y, Wang D, Niu Z, *et al*. A strategy for designing a concave Pt-Ni alloy through controllable chemical etching. Angew Chem Int Ed, 2012, 51: 12524–12528
18 Xu D, Bliznakov S, Liu Z, *et al*. Composition-dependent electrocatalytic activity of Pt-Cu nanocube catalysts for formic acid oxidation. Angew Chem Int Ed, 2010, 49: 1282–1285
19 Lai J, Luque R, Xu G. Recent advances in the synthesis and electrocatalytic applications of platinum-based bimetallic alloy nanostructures. ChemCatChem, 2015, 7, 3206–3228
20 Mavrikakis M, Hammer B, Norskov JK. Effect of strain on the reactivity of metal surfaces. Phys Rev Lett, 1998, 81: 2819–2822
21 Rodriguez J, Goodman DW. The nature of the metal-metal bond in bimetallic surfaces. Science, 1992, 257: 897–903
22 Klimenkov M, Nepijko S, Kuhlenbeck H, *et al*. The structure of Pt-aggregates on a supported thin aluminum oxide film in comparison with unsupported alumina: a transmission electron microscopy study. Surf Sci, 1997, 391: 27–36
23 Richter B, Kuhlenbeck H, Freund HJ, Bagus P. Cluster core-level binding-energy shifts: the role of lattice strain. Phys Rev Lett, 2004, 93: 026805
24 Strasser P, Koh S, Anniyev T, *et al*. Lattice-strain control of the activity in dealloyed core-shell fuel cell catalysts. Nat Chem, 2010, 2: 454–460
25 Stamenkovic VR, Fowler B, Mun BS, *et al*. Improved oxygen reduction activity on Pt_3Ni (111) via increased surface site availability. Science, 2007, 315: 493–497
26 Cui C, Gan L, Heggen M, *et al*. Compositional segregation in shaped Pt alloy nanoparticles and their structural behaviour during electrocatalysis. Nat Mater, 2013, 12: 765–771
27 Tian N, Zhou ZY, Sun SG, *et al*. Synthesis of tetrahexahedral platinum nanocrystals with high-index facets and high electro-oxidation activity. Science, 2007, 316: 732–735
28 Lim B, Jiang MJ, Camargo PHC, *et al*. Pd-Pt bimetallic nanodendrites with high activity for oxygen reduction. Science, 2009, 324: 1302–1305
29 Koh S, Hahn N, Yu CF, Strasser P. Effects of composition and annealing conditions on catalytic activities of dealloyed Pt-Cu nanoparticle electrocatalysts for PEMFC. J Electrochem Soc, 2008, 155: B1281–B1288
30 Stamenkovic VR, Mun BS, Mayrhofer KJJ, *et al*. Effect of surface composition on electronic structure, stability, and electrocatalytic properties of Pt-transition metal alloys: Pt-skin *versus* Pt-skeleton surfaces. J Am Chem Soc, 2006, 128: 8813–8819
31 Mazumder V, Sun SH. Oleylamine-mediated synthesis of Pd nanoparticles for catalytic formic acid oxidation. J Am Chem Soc, 2009, 131: 4588–4589
32 Toda T, Igarashi H, Uchida H, Watanabe M. Enhancement of the electroreduction of oxygen on Pt alloys with Fe, Ni, and Co. J Electrochem Soc, 1999, 146: 3750–3756
33 Zhu HY, Zhang S, Guo SJ, *et al*. Synthetic control of FePtM na-

norods (M = Cu, Ni) to enhance the oxygen reduction reaction. J Am Chem Soc, 2013, 135: 7130–7133
34 Shao Y, Yin G, Gao Y. Understanding and approaches for the durability issues of Pt-based catalysts for PEM fuel cell. J Power Sources, 2007, 171: 558–566
35 Yu X, Ye S. Recent advances in activity and durability enhancement of Pt/C catalytic cathode in PEMFC: part II: degradation mechanism and durability enhancement of carbon supported platinum catalyst. J Power Sources, 2007, 172: 145–154
36 Liu JW, Liang HW, Yu SH. Macroscopic-scale assembled nanowire thin films and their functionalities. Chem Rev, 2012, 112: 4770–4799
37 Cui CH, Li HH, Yu SH. A general approach to electrochemical deposition of high quality free-standing noble metal (Pd, Pt, Au, Ag) sub-micron tubes composed of nanoparticles in polar aprotic solvent. Chem Commun, 2010, 46: 940–942
38 Guo SJ, Zhang S, Su D, Sun SH. Seed-mediated synthesis of core/shell FePtM/FePt (M = Pd, Au) nanowires and their electrocatalysis for oxygen reduction reaction. J Am Chem Soc, 2013, 135: 13879–13884
39 Li HH, Cui CH, Zhao S, *et al*. Mixed-PtPd-shell PtPdCu nanoparticle nanotubes templated from copper nanowires as efficient and highly durable electrocatalysts. Adv Energy Mater, 2012, 2: 1182–1187
40 Mohl M, Dobo D, Kukovecz A, *et al*. Formation of CuPd and CuPt bimetallic nanotubes by galvanic replacement reaction. J Phys Chem C, 2011, 115: 9403–9409
41 Li HH, Ma SY, Fu QQ, *et al*. Scalable bromide-triggered synthesis of Pd@Pt core-shell ultrathin nanowires with enhanced electrocatalytic performance toward oxygen reduction reaction. J Am Chem Soc, 2015, 137: 7862–7868
42 Liang HW, Liu S, Gong JY, *et al*. Ultrathin Te nanowires: an excellent platform for controlled synthesis of ultrathin platinum and palladium nanowires/nanotubes with very high aspect ratio. Adv Mater, 2009, 21: 1850–1854
43 Yin J, Shan S, Yang L, *et al*. Gold-copper nanoparticles: nanostructural evolution and bifunctional catalytic sites. Chem Mater, 2012, 24: 4662–4674
44 Yin YD, Rioux RM, Erdonmez CK, *et al*. Formation of hollow nanocrystals through the nanoscale Kirkendall effect. Science, 2004, 304: 711–714
45 Sun J, Ma H, Jiang H, *et al*. General synthesis of binary PtM and ternary PtM_1M_2 alloy nanoparticles on graphene as advanced electrocatalysts for methanol oxidation. J Mate Chem A, 2015, 3: 15882–15888
46 Wang C, Ren F, Zhai C, *et al*. Au-Cu-Pt ternary catalyst fabricated by electrodeposition and galvanic replacement with superior methanol electrooxidation activity. RSC Adv, 2014, 4: 57600–57607
47 Wang M, He Y, Li R, *et al*. Electrochemical activated PtAuCu alloy nanoparticle catalysts for formic acid, methanol and ethanol electro-oxidation. Electrochim Acta, 2015, 178: 259–269
48 Ferrin P, Mavrikakis M. Structure sensitivity of methanol electrooxidation on transition metals. J Am Chem Soc, 2009, 131: 14381–14389
49 Koh S, Strasser P. Electrocatalysis on bimetallic surfaces: modifying catalytic reactivity for oxygen reduction by voltammetric surface dealloying. J Am Chem Soc, 2007, 129: 12624–12625
50 Garsany Y, Baturina OA, Swider-Lyons KE, Kocha SS. Experimental methods for quantifying the activity of platinum electrocatalysts for the oxygen reduction reaction. Anal Chem, 2010, 82: 6321–6328
51 Guo S, Dong S, Wang E. Three-dimensional Pt-on-Pd bimetallic nanodendrites supported on graphene nanosheet: facile synthesis and used as an advanced nanoelectrocatalyst for methanol oxidation. ACS Nano, 2010, 4: 547–555
52 Rodriguez P, Kwon Y, Koper MTM. The promoting effect of adsorbed carbon monoxide on the oxidation of alcohols on a gold catalyst. Nat Chem, 2012, 4: 177–182
53 Cuesta A. At least three contiguous atoms are necessary for CO formation during methanol electrooxidation on platinum. J Am Chem Soc, 2006, 128: 13332–13333
54 Yamauchi Y, Tonegawa A, Komatsu M, *et al*. Electrochemical synthesis of mesoporous Pt-Au binary alloys with tunable compositions for enhancement of electrochemical performance. J Am Chem Soc, 2012, 134: 5100–5109

Acknowledgements This work was supported by the National Natural Science Foundation of China (21431006), the Foundation for Innovative Research Groups of the National Natural Science Foundation of China (21521001), the National Basic Research Program of China (2014CB931800 and 2013CB931800), the Users with Excellence and Scientific Research Grant of Hefei Science Center of CAS (2015HSC-UE007 and 2015SRG-HSC038), and the Chinese Academy of Sciences (KJZD-EW-M01-1).

Author contributions Fu QQ and Li HH designed and engineered the samples, and wrote the paper; Ma SY helped in data analysis; Fu QQ and Hu BC performed the experiments; Yu SH supervised the project and wrote the paper. All authors contributed to the general discussion.

Conflict of interest The authors declare that they have no conflict of interest.

Supplementary information The evidence of protective capability of HDA; the bulk compositions and surface compositions of different PtAuCu-AA NTs; the composition evolution; TEM images of $Pt_{29}Au_1Cu$ NTs , $Pt_{25}Au_5Cu$ NTs and $Pt_{20}Au_{10}Cu$ NTs and SEAD pattern of $Pt_{27}Au_3Cu$-AA NTs; MOR curves of $(Pt_9Au)_xCu$-AA (x = 2, 3, 4) NTs; XPS patterns of $Pt_xAu_{30-x}Cu$-AA (x = 29, 27, 25, 20) NTs; CV profiles of $Pt_{27}Au_3Cu$-AA NTs during the electrochemical dealloying process; the comparisons of MOR and FAOR mass activity of $Pt_{27}Au_3Cu$ NTs before and after acetic acid treatment; summary of literature catalytic parameters of various Pt-based MOR catalysts; MOR curves and catalyst stability tests of PtCu-AA and $Pt_{27}Au_3Cu$-AA; summary of literature catalytic parameters of various Pt-based FAOR catalysts and long-term stability tests for MOR and FAOR are available in the online version of this paper.

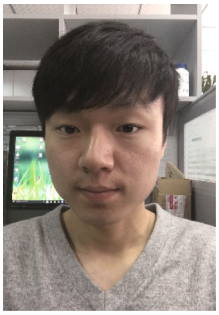

Qi-Qi Fu received his BSc degree majored in chemistry from Lanzhou University, China in 2013. Then he joined the University of Science and Technology of China (USTC) and conducted research under the supervision of Prof. Shu-Hong Yu. His research interest is the synthesis of one-dimensional noble metal alloys as efficient electrochemical catalysts.

Hui-Hui Li received her PhD degree from the USTC in 2014. Currently, she is a post-doctor in Prof. Shu-Hong Yu's group at the USTC. Her research interests include design and synthesis of one-dimensional electrocatalysts. She developed a simple and effective partial sacrificial template method to prepare one-dimensional multi-metallic Pt-based alloy catalysts.

Shu-Hong Yu received his BSc degree at Hefei University of Technology and PhD degree from the USTC. He was a postdoctoral fellow with M. Yoshimura (Tokyo Institute of Technology) and a Humboldt Fellow with M. Antonietti and H. Cölfen (MPI of Colloids and Interfaces, Germany). In 2002, he was appointed the Cheung Kong Professor at the USTC. Currently, he leads the Division of Nanomaterials & Chemistry at Hefei National Laboratory for Physical Sciences at Microscale, USTC. His current research interests include bio-inspired synthesis and self-assembly of new nanostructured materials and nanocomposites, and their related properties. He serves as an editorial advisory board member of journals *Accounts of Chemical Research*, *Chemistry of Materials*, *Chemical Science*, *Materials Horizons*, *Nano Research*, *ChemNanoMat, ChemPlusChem, CrystEngComm*, *Part. Part. Syst. Charact*. and *Current Nanoscience*. His recent awards include *Chem. Soc. Rev*. Emerging Investigator Award (2010) and Roy-Somiya Medal of the International Solvothermal and Hydrothermal Association (ISHA) (2010).

在混合溶剂中以铜纳米线为模板制备高效双功能三元PtAuCu纳米管电催化剂

傅棋琪, 李会会, 马思阅, 胡必成, 俞书宏

摘要 与非贵金属形成合金是一种能大幅减少电催化剂中贵金属用量的有效方法, 且形成合金有利于催化性能提升. 本文引入了一种混合溶剂体系, 通过采用高质量铜纳米线作为部分牺牲模板合成了多孔均一、表面粗糙的PtAuCu三元纳米管. 实验表明金的引入是催化剂甲醇氧化(MOR)和甲酸氧化(FAOR)性能提升的一个关键因素. 其MOR和FAOR质量活性分别达到了1698.8 mA mg^{-1}_{Pt}(0.9V)和1170 mA mg^{-1}_{Pt}(0.65V). 由于CO^{*}不可逆的吸附在金的表面而非有催化活性的铂表面, 这种三元纳米管催化剂表现出了优异的催化稳定性和结构稳定性. 此外, 这种合成方法可以用于合成其他的新型双功能催化剂.